

Multiphysical Analysis of High Torque Density Propulsion Motors for E-mobility Applications

Sándor HORVÁTH, Kristóf KISS, István VAJDA

Széchenyi István University, Győr, Hungary
Electromobility Research Center
e-mail: sandor.horvath@pm.me

E-mobility is one the most demanding applications for rotating electrical machines in our present days. A typical duty includes not only non-periodic load and speed variations, but frequent overloads and changeovers between motoring and regenerative braking as well. To achieve competitiveness, an integrated electric powertrain has to face strict technical-economic requirements. These can only be fulfilled by applying high torque density propulsion motors. The utilization of a given electrical machine is generally expressed by its Torque per Rotor Volume (TRV) ratio. In order to protect the insulation system from overheating and thus lifetime reduction or critical failure, the maximum permissible value for TRV very much depends on the intensity of cooling. Further design aspects like mechanical stresses and deformations, envelope dimensions, efficiency requirements, limited weight of active and inactive parts also influence the achievable or allowable utilization. Software packages for industrial purposes provide great functionality with ease of use. However, for academic and research interests, often more flexible and transparent modeling and evaluation techniques are needed. At the Electromobility Research Center, Authors are developing a software tool to perform rapid multiphysical analysis on various propulsion motor types, equipped with different liquid-cooling methods. This Paper introduces the modeling and simulation processes, which have been implemented for sinusoidal supply machines with radial fluxpath and inner rotor so far.

Keywords: *electric propulsion, multiphysics, self-developed software, co-simulation*

1 Electromagnetic Topology Analysis

1.1 Software Concept and Implementation

Throughout various fields of engineering, topology optimization is a novel approach for problems of distributing a limited amount of material in a design space, by satisfying predefined objectives and constraints. To obtain practical solutions,

with regards to manufacturability, advanced methods are being recently implemented for different types of rotating electrical machines [1], [2].

The Electromagnetic Topology Analyser (EMTA), presented in this Paper, is a self-developed software tool for automated characterization of propulsion motor alternatives, like Squirrel Cage Induction Machine, Permanent Magnet Synchronous Machine, Switched Reluctance Machine and Synchronous Reluctance Machine. Topology refers to the combination of core geometry, material properties and winding scheme, being a simplified numerical representation of the physical machine. Operation of EMTA is based on a connection between a finite element software – capable of field simulation – and a high-level control environment. Block diagram of EMTA, indicating the software components, is shown in Fig. 1.1.

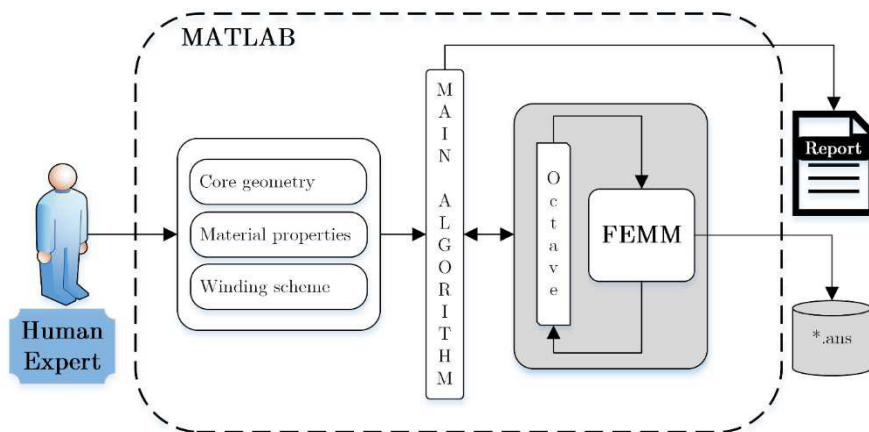


Fig. 1.1. System diagram of Electromagnetic Topology Analyser and the selected components

According to Fig. 1.1., the high-level control was implemented in MATLAB 8.5 environment, while FEMM v4.2 was chosen as the finite element software.

FEMM is a suite of programs for solving low frequency electromagnetic problems on two-dimensional planar and axisymmetric domains. The v4.2 addresses linear/nonlinear magnetostatic problems, linear/nonlinear time harmonic magnetic problems, linear electrostatic problems, and steady-state heat flow problems [3]. Octave is practically an interface, which enables the automation of FEMM via a predefined set of MATLAB-functions. The syntax of an Octave program is similar to that of FEMM's Lua scripting language, but is more powerful due to the matrix-oriented nature of MATLAB. Octave distribution is installed with FEMM v4.2 [4].

At the beginning of a new topology analysis process, the Human Expert has to choose between available machine types and enter the corresponding input data, based on physical dimensions. Main Algorithm is a complex MATLAB routine,

with separate modules for different machine types, which were design to be interchangeable. Topological similarities can be exploited due to this modular structure. While the Human Expert is an organic component of this system, to eliminate time-consuming repetitive human work and interaction, numerous automatisms were implemented:

- definition of the EM problem, boundary and symmetry conditions;
- model assembly (geometry + material properties + winding scheme);
- control of spatial discretization and solver algorithms;
- effective utilization of computational resources;
- raw data management and post-processing;
- extracting and storing useful information, visualization, data sharing.

FEMM is capable of certain post-processing tasks, which are also controlled and extended by the Main Algorithm. By default, all *.ans result files are stored, giving the possibility of additional data extraction in future. At the end of a topology analysis sequence, results get summarized for the Human Expert in a *.pdf Report file. FEMM was chosen as the core software component for EMTA because of its simple usability and detailed documentation for automation. A similar application, with a coupling between MATLAB and FEMM, is mentioned in [6] for SynRM.

1.2 Modeling and Simulation

To demonstrate analysis capabilities, an embedded-type PMSM was designed with a reasonable TRV ratio, approximately 85% of Nissan Leaf's peak torque density [5]. The specification includes the following requirements and constraints:

- Configuration: radial flux path, inner rotor, no field-weakening mode
- Total volume: 5 litres (SOD=240 mm and L=110 mm)
- Peak TRV $\approx 120 \text{ kNm/m}^3 \rightarrow \text{SID}=170 \text{ mm}$, stator with 48 slots
- Hypothetical operating temperature: 110 °C ; Ambient temperature: 20 °C
- Winding: 16 poles, max. 50% effective slot fill factor
- Core material: M350-50A
- PM material: N41UH ($H_c = -906 \text{ kA/m}$; $B_r = 1.17 \text{ T}$ at 110 °C)

As one may notice, a relatively commercial core material was selected, in order to obtain practical solutions. The rare-earth PM material was chosen to provide a competitive energy-product, yet capable of withstanding ultra high temperature. No field-weakening mode is required, meaning that a horizontal PM arrangement is suitable for the embedded-type rotor. Neither bridges and ribs in the rotor lamination, nor PM dimensions were optimized in the reference design.

For geometrical modeling of a given topology, point with Cartesian-coordinates are assigned to certain points of the lamination layout. This way, geometry can be easily manipulated. By increasing the number of these reference points, we have the possibility to create complex geometries with various transitions (chamfers, fillets). Time demand of simulation increases due to geometrical complexity.

During a topology analysis, often hundreds of individual electromagnetic problems must be solved. In case of a synchronous machine, e.g. to obtain detailed torque characteristics, a locked-rotor test is simulated at different positions (at their corresponding load-angles) for a current source feeding, via magnetostatic analysis. The Main Algorithm organizes these individual problems into a sequence.

For meshing, i.e. discretization of the solution region by thousands of simple shapes, *triangle.exe* is applied by default. Mesh density, i.e. the number of nodes and their size, is crucial in terms of calculation accuracy and time demand. In a region of high gradients, like the airgap of rotating machines, mesh should be set properly dense. Applied mesh density for the reference design can be seen in Fig. 1.1. below.

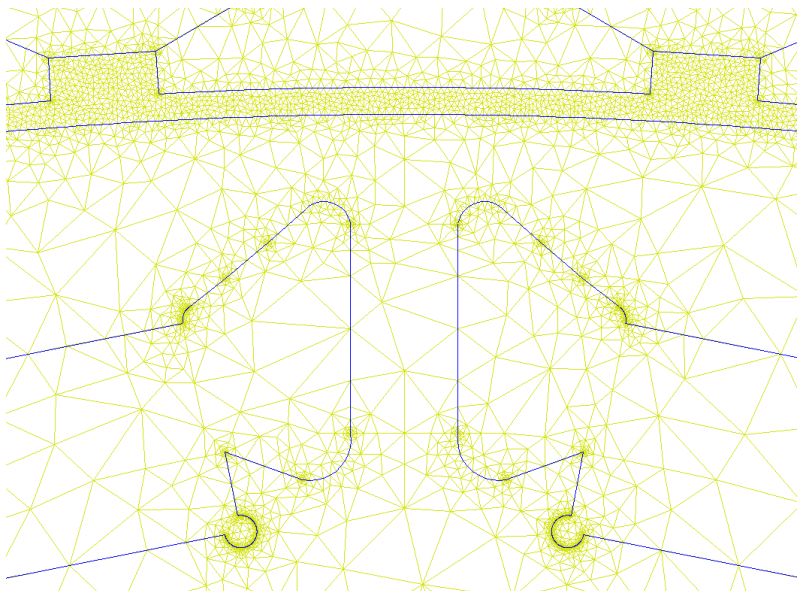


Fig. 1.2. Applied mesh density in the vicinity of air gap, before PM insertion

Effective utilization of computational resources was carried out by a multithreaded programming technique, via the parallelization of solver instances. By applying this MATLAB feature, the time demand of an analysis sequence can be significantly reduced for magnetostatic problems, as linear function of physical processor cores.

The relevant partial differential equations for all nodes are solved by fkern.exe. Both triangle.exe and fkern.exe are integrated components of FEMM v4.2.

According to the electromagnetic finite element calculation, the required peak TRV ratio ($\approx 120 \text{ kNm/m}^3$) can be reached by applying an electrical overload.

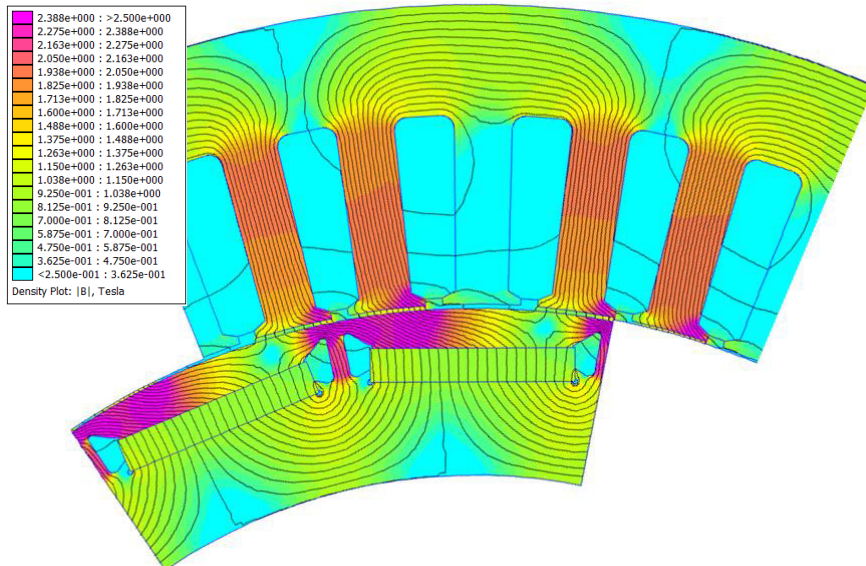


Fig. 13. Full-load flux-density plot for the modeled fraction

The reference design produces 300 Nm air gap torque at 120 kArms/m linear current density. Current density in the conductors is 22.5 A/mm^2 .

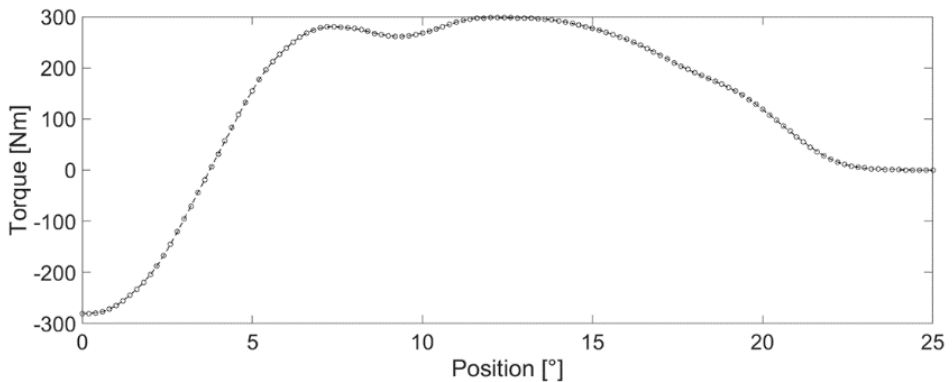


Fig. 14. Full-load torque-characteristics

Input geometry, loads and losses are then transferred to the thermal analysis modul.

2 Transient Thermal Topology Analysis

2.1 Software Concept and Implementation

A thermal model based on Beuken's RC-analogy was built in Matlab. The model is capable of calculating the temperature distribution of the stator when geometrical, cooling and load parameters are given.

The program starts with loading the model settings and parameters of the input geometry. Model settings define the chosen node density of the model, while the input geometry contains the dimensions of the stator. Then a test program is loaded, which defines the load characteristics in time. In the recent software version, only constant load is supported.

After storing the needed geometry, the list of materials used in the model are loaded. The geometry, the materials and their properties are contained in Matlab structures, 'structs' on the global workspace. For example the electrical steel is contained under the name of 'Iron', with the following properties:

- Specific heat
- Mass density
- Electrical conductivity
- Thermal conductivity in d,q and h directions
- Thermal coefficient of losses
- Hysteresis coefficient for loss calculation

As a lumped parameter thermal model requires the thermal nodes to be homogenous or quasi-homogenous, node size would need to be greatly reduced for the slot, for it contains a multitude of materials. Another approach we followed is to create an equivalent slot material based on the Hashin-Shtrikman approximation. [7] Although the approximation is described for a two-component system, we used a weighted average to calculate the equivalent insulation parameters (λ_p, c_p), and then, the equivalent slot parameters (λ_e, c_e) using the following formulae:

$$\lambda_e = \lambda_p \frac{(1 + v_c)\lambda_c + (1 - v_c)\lambda_p}{(1 - v_c)\lambda_c + (1 + v_c)\lambda_p} \quad [2](1)$$

$$c_e = \frac{v_c(\rho_c c_c - \rho_p c_p) + \rho_p c_p}{v_c(\rho_c - \rho_p) + \rho_p} \quad 2$$

Where v_c is the copper fill factor, ρ_p, ρ_c are the insulation and copper mass densities, respectively. The equivalent conductivity λ_e is valid in d and q (radial and tangential) directions. The axial conductivity is considerably higher – as there is continuous copper winding to conduct heat – it was chosen to be equal to the

conductivity of copper multiplied by the fill factor. This induces a negligible error because of the difference between material conductivities. [8]

The method for creating a quasi-homogenous material is erroneous when calculating with higher fill factors, showing a higher equivalent conductivity than numerical simulations and measurements of [7] showed. It is also computes a higher conductivity value when there is considerable difference between the conductivity values of the different insulating materials. It is, however, more accurate in calculating heat capacity than numerical models.

Once material properties are defined, a thermal network is to be created. For defining a thermal network, the object needs to be separated to finite volumes with simple geometries. In case of rotating machines, the simplest geometry is a cylindrical section, shown by Fig. 2.1. These simple geometries called thermal cells [8] or nodes [9], and they also need to be homogenous, as mentioned before.

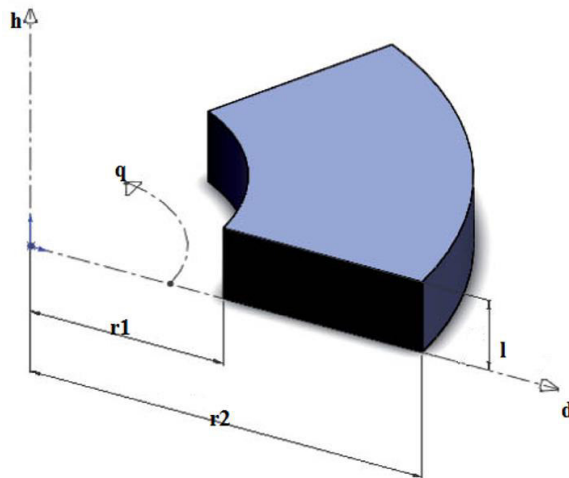


Fig. 2.1. Thermal cell definition for a simple cylindrical section

When these requirements are fulfilled, the thermal properties of these nodes can be calculated. This is the point where the advantages of lumped parameter models are noticeable: even with higher node count, the computation remains fast. This is because the simple geometries allow one to use a linear system of equations based on the result of the differential equation of heat transfer, rather than needing to solve the differential equation itself. One obvious disadvantage is also noticeable: it is tedious to create certain geometries, models often require simplifications.

The basic solution for the thermal conductivity of a cylindrical body:

$$K_D = \frac{\lambda_d \cdot q}{\log\left(\frac{r_2}{r_1}\right)}; \quad K_Q = \frac{\lambda_q \cdot \log\left(\frac{r_2}{r_1}\right)}{q}; \quad K_H = \frac{\lambda_h \cdot (r_2^2 - r_1^2) \cdot q \cdot \frac{\pi}{2}}{l} \quad [2](3)$$

In addition to conductivity values between two nodes, the heat capacities and nodal losses also need to be defined. Heat capacity is calculated by multiplying specific heat capacity and mass density values of materials by node volume.

External temperature and surface heat transfer coefficient can be set arbitrarily.

2.2 Importing Losses from 2D Electromagnetic Analysis

Nodal losses are gained by summing all losses inside their finite volume. For this reason it is advantageous to define specific losses as well. A specific loss value for copper losses is given as follows:

$$p_{Cu} = J^2 \cdot \frac{ff_{Cu}}{\sigma_{Cu}} \cdot k_R \quad [2](4)$$

Where J is the current density flowing in the copper conductor, ff_{Cu} the fill factor of copper in slot, σ_{Cu} is the electrical conductivity of copper, and k_R is a coefficient describing increased losses due to alternating current (depending on material parameters, slot geometry and supply frequency). [9] With this method, the geometrical and material input values are defined. The current density, as electrical load comes from the 2D electromagnetic solution. Copper loss for each node can be calculated by multiplying p_{Cu} with the node volume.

A similar approach is used with iron losses, where the source is, once again, the electromagnetic solution. This time the relevant source is the flux density map and the supply frequency. When multiple time steps are calculated, the time function of average flux density is extracted for each node. With the time functions and base frequency available, a Fourier transform is performed and the following expressions are evaluated to obtain $p_{Fe,EC}$ eddy current and $p_{Fe,Hy}$ hysteresis loss.

$$p_{Fe,EC} = \frac{\pi^2}{6} \cdot \sigma_{Fe} \cdot f^2 \cdot d^2 \cdot \sum_{n=1}^{\infty} n^2 B_n^2 \quad [2](5)$$

$$p_{Fe,Hy} = C_{Hy} \cdot \frac{f}{\rho_{Fe}} \cdot \sum_{n=1}^{\infty} n^2 B_n^2 \quad [2](6)$$

Where σ_{Fe} , ρ_{Fe} , C_{Hy} are the electric conductivity, mass density and hysteresis coefficient of lamination material, d is lamination thickness and f is base frequency of supply, respectively. [9] The specific iron losses are to be multiplied by node volume to acquire nodal losses – with the difference of even specific iron losses being differentiated node by node.

An easier solution is importing a single flux density solution, sweeping it by the radius and collecting the highest flux density absolute value for each specific radius. Then, assuming a sinusoidal flux distribution the losses are calculated with the above mentioned [2](5)-[2](6) equations. This assumption greatly decreases computational requirements, but reduces accuracy at the same time.

2.3 Modeling and Simulation

Correctly defining the finite volumes of the machine and creating a thermal conductance matrix is the most time-consuming part of creating a lumped parameter model. For every new topology the method requires a new matrix, in other words, a completely new model. Our goal was to create a system where building a model is as fast as possible. Using Matlab structures, thermal nodes are built. The input of a builder function for a cylindrical element requires the outer and inner radius, length and angle of the cylindrical section, the material and the loss flag to be used. Loss flags guide the program on which loss equation to use later. The structure of a machine part consists of the following elements:

- Heat Transfer Matrix
- Vector containing Volume of nodes
- Vector containing Heat capacity of nodes
- Vector containing Loss flag of nodes
- Vector containing Cooled flag of nodes
- Vector containing Cooling direction flag of nodes
- 6 Vectors containing conductivity values towards neighboring machine parts or the environment (one for each spatial dimension and direction)
- 6 Vectors containing the list of nodes that are connected with the environment
- 4 Vectors containing Surface area of nodes
- A struct containing geometry of nodes

A heat transfer matrix describes thermal connections between nodes of a model. If the i -th and j -th node are directly thermally connected, the matrix will contain the thermal conductivity value between them with a negative sign in its ij and ji elements. [3] The main diagonal is empty at this point.

After the basic structures are defined, they are to be joined, in order to create more complex geometries. Joining two structures means concatenating their matrices and vectors, as well as completing the thermal conductivity matrix by new elements, which describe connections between the two structs. If during joining some nodes have their material property described as 'coolant', they will not appear in the heat transfer matrix, the neighboring nodes will have their 'cooled' flag enabled instead.

Fig. 2.2.(a) shows the heat transfer matrix and the modeled part of the machine it represents. The model is built from 800 nodes and 3088 thermal connections are defined. The coloring of Fig. 2.2.(b) represents loss flags: blue for no loss, green for iron loss and yellow for copper loss.

Once the whole model is built, the losses are calculated for each node and the main diagonal of the heat transfer is filled according to the following rule:

$$K_{ii} = K_{i,0} - \sum_{k=1}^n K_{i,k} - \beta_i \cdot P_i \quad [2](7)$$

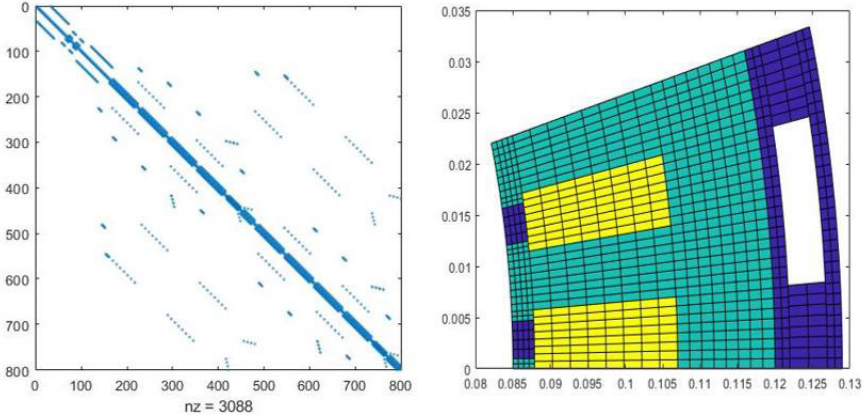


Fig. 2.2. (a) Heat transfer matrix ; (b) Modeled machine fraction, indicating losses

Where $K_{i,l}$ is the thermal conductivity towards the coolant or environment, if there is any, $\sum_{k=1}^n K_{i,k}$ is the sum of conductivity values between the i -th node and other nodes. $\beta_i * P_i$ is a correction factor for temperature-dependent losses (β_i is the temperature coefficient of loss and P_i is the loss in the i -th node).

Specific losses were calculated in the previously discussed manner for the reference design, at a low speed, maximum torque operating point. See Fig. 2.3. for details.

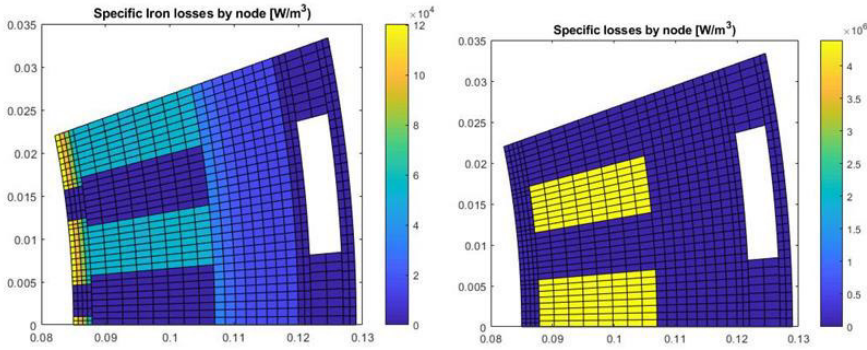


Fig. 2.3. (a) Specific iron losses ; (b) Specific copper losses

With the heat transfer matrix complete and the vector containing the losses ready the linear equation for thermal transients can be solved.

$$\vec{T}_{\tau+1} = \left(\frac{2 * \text{diag}\{\vec{C}\}}{\Delta\tau} + \mathbf{K} \right) \setminus \left\{ \vec{P}_{loss} \left(1 + \vec{\beta}(\vec{T}_{\tau} - T_{\beta}) \right) + \vec{K}_0 \vec{T}_{amb} + \frac{2\vec{C}}{\Delta\tau} \vec{T}_{\tau} \right\} \quad [2](8)$$

Where \vec{T} is the Vector of nodal temperatures, \vec{C} is the Vector of nodal heat capacitances, \mathbf{K} is the Heat transfer matrix, $\Delta\tau$ is the time step of choice, \vec{P}_{loss} is the Vector containing the nodal losses, $\vec{\beta}$ is the Temperature dependence vector of losses, \vec{T}_{amb} ambient temperature and \vec{K}_0 is heat transfer towards the environment.

The solution for the hot-spot temperature is seen on Fig. 2.4.(a). The steady-state temperature is much higher than acceptable – the electromagnetic load is greater than what cooling capabilities would allow in continuous operation. (The calculated operating point was a forced, peak torque transient-state). It should also be noted, that the end winding, which has usually weaker cooling [10], was not modeled.

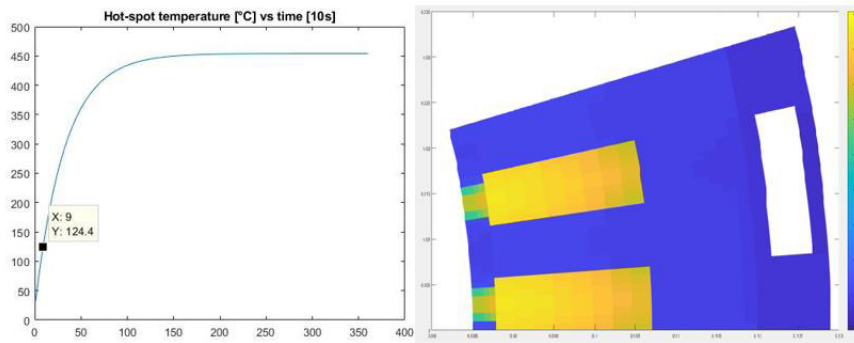


Fig. 2.4. (a) Hot-spot temperature: 124.4 °C after 90 sec ; (b) Temperature distribution after 80 seconds

The hypothetically allowed 110°C hot-spot temperature for the discussed reference design, under the given conditions, was reached in approximately 80 seconds.

4 Conclusion

The presented software tool is capable of performing a rapid and computationally efficient coupled analysis, considering electromagnetic and thermal domains with one-way data transfer. A more sophisticated multiphysical approach would use two-way data sharing, in order to take the changing material properties during a forced transient operation into account. In the recent software version, only stator losses are mapped to the thermal domain, meaning that so far the application is limited to permanent magnet synchronous and various kind of reluctance machines. Further development plans includes not only total validation, but extending capabilities to squirrel cage induction machine analysis as well. From the user's point of view, a graphical user interface should also be implemented in the future.

Development of a Multiphysical Topology Optimizer tool is a long-term goal for the Authors, e.g. to improve torque characteristics of prospering synchronous reluctance machines, similarly to [11]. However, practical improvements can only be made after detailed validation of presented methods.

5 Acknowledgement

Authors would like to express their gratitude to the Electromobility Research Center at Széchenyi István University, for supporting their ambitions and interest related to novel electric powertrain and propulsion motor development.

References

- [1] Sato, T. ; Watanabe, K. ; Igarashi, H.
Multimaterial Topology Optimization of Electric Machines Based on Normalized Gaussian Network
IEEE Transactions On Magnetics, 51(3): 7202604, 2015
- [2] Jung, S-W. ; Ro, J-S. ; Jung, H-K.
A Hybrid Algorithm Using Shape and Topology Optimization for the Design of Electric Machines
IEEE Transactions On Magnetics, 54(3): 8102604, 2018
- [3] Meeker, D.
Finite Element Method Magnetics v4.2 : User's Manual
<http://www.femm.info/Archives/doc/manual.pdf>, 2015
- [4] Meeker, D.
Finite Element Method Magnetics – OctaveFEMM v1.2 : User's Manual
<http://www.femm.info/Archives/doc/octavefemm.pdf>, 2010
- [5] Staton, D. ; Goss, J.
Open Source Electric Motor Models for Commercial EV & Hybrid Traction
https://www.coilwindingexpo.com/berlin/__media/pages/Tutorial-1-D--Staton-&-J--Goss-MDL.PDF , CWIEME 2017
- [6] Pellegrino, G. ; Cupertino, F. ; Gerada, C.
Automatic Design of Synchronous Reluctance Motors Focusing on Barrier Shape Optimization
IEEE Transactions On Industry Applications, 51(2): 15000375, 2015
- [7] Imre, L.
Villamos gépek és eszközök melegedése és hűtése
Műszaki Könyvkiadó, Budapest, 1982
- [8] Pyrhonen, J. ; Jokinen, T. ; Hrabovcova, V.
Design of Rotating Electrical Machines 2nd Ed.
Wiley, 2013

- [9] Krings, A.
Iron Losses in Electrical Machines – Influence of Material Properties,
Manufacturing Processes, and Inverter Operation
KTH Stockholm, 2014

- [10] Simpson, N. ; Wrobel, R. ; Mellor, P.H. ;
Estimation of Equivalent Thermal Parameters of Impregnated Electrical
Windings
IEEE Transactions On Industry Applications, 49(6): 13914355, 2013

- [11] Okamoto, Y. et al.
Improvement of Torque Characteristics For a Synchronous Reluctance
Motor Using MMA-based Topology Optimization Method
IEEE Transactions On Magnetics, 54(3): 7203104, 2018